

Exclusive electroproduction of strange mesons with JLab 12 GeV*

M. Strikman

Department of Physics, Pennsylvania State University, University Park, PA 16802, USA

C. Weiss

Theory Center, Jefferson Lab, Newport News, VA 23606, USA

We summarize the physics topics which can be addressed by measurements of high- Q^2 exclusive electroproduction of strange mesons, $\gamma^*N \rightarrow \phi N, K^*\Lambda, K\Lambda, K\Sigma$, at Jefferson Lab with 11 GeV beam energy. The proposed investigations are aimed both at exploring the reaction mechanism (dominance of point-like configurations) and extracting information about baryon structure from the data (generalized parton distributions, or GPDs). They include (a) probing the t -dependence of the nucleon's gluon GPD (transverse spatial distribution of gluons) in ϕ meson production; (b) separating the nucleon helicity-flip and nonflip quark GPDs in $K^*\Lambda$ production with measurement of the Λ recoil polarization; (c) probing strangeness polarization in the nucleon in $K\Lambda$ and $K\Sigma$ production. These studies rely only on the analysis of cross section ratios, which are less affected by the theoretical uncertainties of present GPD-based calculations than absolute cross sections.

I. INTRODUCTION

Exclusive electroproduction of mesons, $\gamma^*N \rightarrow MN'$, at energies above the resonance region, $W > 2$ GeV, and low momentum transfer to the nucleon, $|t| \lesssim 1$ GeV², offers many interesting opportunities for studying strong interaction dynamics as well as baryon and meson structure at variable resolution scale, defined by the photon virtuality, Q^2 . At low virtualities, $Q^2 \lesssim 1$ GeV², such reactions are conventionally described in terms of hadronic fluctuations of the virtual photon and their interaction with the target. At high virtualities, $Q^2 \gg 1$ GeV², the production process becomes effectively point-like and can be described as the interaction of the virtual photon with partonic degrees of freedom in the target. In the asymptotic regime, a QCD factorization theorem [1] allows one to calculate the electroproduction amplitudes in terms of the generalized parton distributions (GPDs) of the target (more precisely, of the $N \rightarrow N'$ transition) and the distribution amplitudes (DAs) of the produced meson M — universal characteristics of the quark and gluon structure of the hadrons, which are probed also in other hard scattering processes such as inclusive DIS, elastic scattering, and e^+e^- annihilation (see Refs. [2, 3, 4] for reviews).

The analysis of such processes at high Q^2 typically proceeds in two stages. In the first stage, one tries to ascertain the approach to the point-like regime by testing certain qualitative features which do not depend on the specific form of the GPDs/DAs and the details of the hard scattering process (examples of such tests will be given below). In the second stage, one may then try to extract quantitative information about the GPDs and/or DAs by comparing suitable process observables with correspond-

ing theoretical predictions calculated assuming factorization. Of particular interest is the fact that a given meson channel probes specific quantum numbers of the $N \rightarrow N'$ transition GPD, making it possible to separate different spin/flip components and perform comparative studies of related channels. While the practical applicability of the factorized approximation to meson production at $Q^2 \sim \text{few GeV}^2$ is far from established, and most likely requires substantial sub-asymptotic corrections (“higher twist”), the study of such processes can in principle contribute much valuable information to the GPD analysis.

In this article we attempt to summarize which questions could be addressed by measurements of high- Q^2 exclusive electroproduction of strange mesons, in the kinematic region accessible with the 12 GeV Upgrade of Jefferson Lab. Our survey covers three main channels, each of which has its own distinctive physical interest and potential use in the GPD analysis:

$$\gamma^*N \rightarrow \phi N, \quad (1)$$

$$\gamma^*p \rightarrow K^{*+}\Lambda, \quad (2)$$

$$\gamma^*p \rightarrow K^+\Lambda, K^+\Sigma^0, K^0\Sigma^+. \quad (3)$$

ϕ meson production, Eq. (1), allows one to investigate the approach to the point-like regime through the transverse momentum transfer dependence of the cross section, and to study the t -dependence of the nucleon's gluon GPD and obtain information about the transverse spatial distribution of gluons (Sec. III). Production of $K^*\Lambda$ with measurement of the transverse recoil polarization, Eq. (2), can be used to separate the helicity-flip and nonflip components of the $N \rightarrow \Lambda$ transition GPDs, complementing measurements with a transversely polarized target. Even more information on the helicity structure could be obtained by combining target and recoil polarization. In these experiments σ_L and σ_T can effectively be separated by analyzing the angular distribution of the vector meson decay and relying on s -channel helicity conservation; this method avoids comparing data at different beam energies, which is costly and limits the

*Prepared for the CLAS 12 RICH Detector Workshop, January 28–29, 2008, Jefferson Lab, Newport News, VA, USA; <http://conferences.jlab.org/clas12/>.

kinematic reach of the experiments. Further information about the flavor structure of quark GPDs can be gained from measurements of the ratio of $K^{*+}\Lambda$ and ρ^+n production cross sections (Sec. IV). Finally, $K\Lambda$ and $K\Sigma$ production Eq. (3), are sensitive to the polarized $N \rightarrow N'$ transition GPDs \tilde{H} and \tilde{E} , which by $SU(3)$ flavor symmetry can be related to the strangeness polarization in the nucleon (Sec. V).

An essential point is that the investigations described here rely on the analysis of cross section ratios rather than absolute cross sections. As explained in Sec. II, present GPD-based calculations of absolute meson production cross sections at JLab energies suffer from considerable theoretical uncertainties. Measurements of cross section ratios, in which these uncertainties cancel at least partly, presently seem to be the best option for utilizing meson production for the GPD analysis at JLab 12 GeV. One may hope, of course, that progress in the theory and phenomenology of exclusive meson production would eventually allow us to analyze also absolute cross section observables in these processes.

In strange meson electroproduction at high Q^2 the cross sections for processes with transition to decuplet baryon transitions are generally of the same order as those for octet baryons. This makes it possible to use hard exclusive processes of the type discussed here as a new tool in resonance spectroscopy. While not the main focus of this summary, we comment on this interesting option in Secs. II and VI.

II. THEORETICAL STATUS OF HIGH- Q^2 MESON PRODUCTION

The theoretical basis for the analysis of processes such as Eqs. (1)–(3) at high Q^2 is the QCD factorization theorem for hard exclusive meson electroproduction [1]. At $Q^2 \gg R_{\text{hadron}}^{-2}$, the meson is produced in a configuration much smaller than its typical hadronic size. The amplitude for longitudinal (L) photon polarization can be factorized into a hard scattering process, calculable in perturbative QCD, the $N \rightarrow N'$ transition GPD, describing the emission/absorption of the active parton (quark or gluon) by the nucleon, and the DA of the produced meson, describing the hadronization of the outgoing $q\bar{q}$ pair (see Fig. 1). Factorization in these processes is closely related to the phenomenon of color transparency — the fact that color-singlet configurations of size $r \ll R_{\text{hadron}}$ interact weakly with hadronic matter; this connection is seen most clearly when following the space-time evolution of the reaction in the target rest frame [5].

There are many indications for substantial corrections to the asymptotic reaction mechanism at momentum transfers $Q^2 \sim \text{few GeV}^2$, originating from production of the meson in configurations of finite size $1/Q \ll r \lesssim R_{\text{hadron}}$. In the kinematic region of $x_B \ll 10^{-1}$, clear evidence for such corrections comes from the Q^2 -dependence of the t -slopes of several vector meson pro-

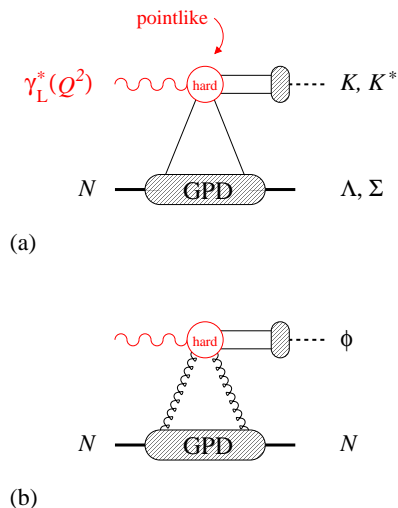


FIG. 1: QCD factorization in exclusive electroproduction of strange mesons. K and K^* production (a) probe nonsinglet quark GPDs, ϕ production (b) mostly the gluon GPD.

duction channels ($\rho^0, \phi, J/\psi$) measured at HERA (see Ref. [5] for details). The t -slope, which at small x_B coincides with the slope in the transverse momentum transfer to the target, Δ_{\perp}^2 (see Sec. III), measures the total transverse size of the interaction region, as determined by the size of the relevant configurations of the target and the produced meson, and becomes Q^2 -independent in the asymptotic regime where the meson is produced in a point-like configuration (see Fig. 2). The data show that ρ^0 and ϕ slope still decrease up to $Q^2 \approx 10 \text{ GeV}^2$, indicating that there is still a significant contribution from finite-size configurations [5]. It is worth emphasizing that this observation could not possibly be explained by higher-order QCD corrections and must be attributed to finite-size effects. (Next-to-leading order QCD corrections to meson production amplitudes were studied in Refs. [6].) Further evidence for finite-size effects, more pertinent to the kinematic region of $x_B \gtrsim 10^{-1}$ relevant to JLab, comes from the extensive studies of the pion

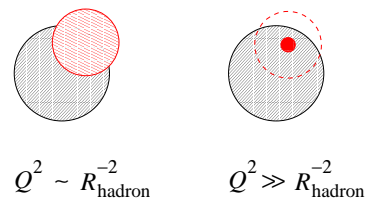


FIG. 2: The transverse spatial structure of the interaction region in meson production at $Q^2 \sim R_{\text{hadron}}^{-2}$ (left) and $Q^2 \gg R_{\text{hadron}}^{-2}$ (right). The photon virtuality determines the effective transverse size of the configurations in which the meson is produced. Experimentally, the transverse size of the interaction region is reflected in the t -slope (more precisely, the Δ_{\perp}^2 -slope) of the differential cross section.

form factor at high Q^2 , whose asymptotic behavior is governed by a hard scattering mechanism closely related to high- Q^2 exclusive meson production (see Refs. [4, 7] for reviews). In fact, the charged pion/kaon production amplitude contains a “pole term” governed by the pion/kaon form factor (see Sec. V), and the findings about finite-size effects in the pion form factor directly impact on the GPD-based description of meson production.

In theoretical calculations of meson production cross sections based on QCD factorization one faces several questions: (a) how to model the GPDs; (b) how to treat the hard scattering process (choice of scale in α_s , higher-order corrections); (c) how to consistently combine contributions from meson production in small-size and large-size configurations. While in theory these are distinct questions which can be discussed separately, in practice the issues are closely related, implying that the approximations made in the treatment of one will generally influence the conclusions one draws about the others. The situation is reasonably well under control in vector meson production at collider energies (HERA, EIC), where the dominant gluon GPD can be reconstructed at $t = 0$ from the usual gluon density in a well-controlled approximation, and the finite size of the produced meson (intrinsic transverse momentum) can be incorporated phenomenologically in the dipole picture in space-time, justified by the large coherence length of the process, $l_{\text{coh}} \sim 1/(2M_N x_B) \gg 1 \text{ fm}$ [8]. (Another approach to finite-size effects at small x_B , based on intrinsic transverse momentum, was pursued in Ref. [9].) In the kinematics of fixed-target experiments (HERMES, JLab) the situation is generally more complicated. Present model calculations of absolute meson production cross sections in this region show considerable uncertainty (see *e.g.* Refs. [10, 11]). Progress can be expected from further theoretical studies of the reaction mechanism (space-time picture, real vs. imaginary part of the amplitude), as well as from fully differential cross section measurements (t - and W -dependences for given Q^2 ; L/T separation and other response functions, polarization observables) with JLab 12 GeV.

Given the present uncertainties in GPD-based calculations of absolute meson production cross sections, a reasonable approach is to concentrate on the analysis of cross section ratios in which these uncertainties cancel at least to some extent. Such “ratio observables” can be used either to test certain qualitative predictions of the approach to the point-like regime, or to extract specific information about the GPDs. Examples are:

- The t -dependence of the cross section and its change with Q^2 , which measures the transverse size of the interaction region and the t -dependence of the GPDs;
- Target and recoil polarization asymmetries, which can be used to separate the nucleon helicity components of the GPDs;
- Beam single-spin and beam + target double-spin

$\rho^0 p$	$\frac{1}{\sqrt{2}}[2u + d] + \frac{1}{\sqrt{2}}[2\bar{u} + \bar{d}] + \frac{3}{4}g$
ωp	$\frac{1}{\sqrt{2}}[2u - d] + \frac{1}{\sqrt{2}}[2\bar{u} - \bar{d}] + \frac{3}{4}g$
ϕp	$-[s + \bar{s}] + \frac{3}{4}g$
$\rho^+ n$	$2[u - d] - [\bar{u} - \bar{d}]$
$K^{*+} \Lambda$	$-\frac{2}{\sqrt{6}}[2u - d - s]$ $+ \frac{1}{\sqrt{6}}[2\bar{u} - \bar{d} - \bar{s}]$
$K^{*+} \Sigma^0$	$-\frac{2}{\sqrt{2}}[d - s] + \frac{1}{\sqrt{2}}[\bar{d} - \bar{s}]$
$K^{*0} \Sigma^+$	$[d - s] + [\bar{d} - \bar{s}]$
$\pi^+ n$	$2[\Delta u - \Delta d] + [\Delta \bar{u} - \Delta \bar{d}]$
$\pi^0 p$	$\frac{1}{\sqrt{2}}[2\Delta u + \Delta d] - \frac{1}{\sqrt{2}}[2\Delta \bar{u} + \Delta \bar{d}]$
$K^+ \Lambda$	$-\frac{2}{\sqrt{6}}[2\Delta u - \Delta d - \Delta s]$ $-\frac{1}{\sqrt{6}}[2\Delta \bar{u} - \Delta \bar{d} - \Delta \bar{s}]$
$K^+ \Sigma^0$	$-\frac{2}{\sqrt{2}}[\Delta d - \Delta s] - \frac{1}{\sqrt{2}}[\Delta \bar{d} - \Delta \bar{s}]$
$K^0 \Sigma^+$	$[\Delta d - \Delta s] - [\Delta \bar{d} - \Delta \bar{s}]$

TABLE I: Spin/flavor combination of GPDs entering in the amplitudes of hard exclusive vector (top) and pseudoscalar (bottom) meson production with proton target, $\gamma^* p \rightarrow MN'$, assuming $SU(3)$ flavor symmetry [2, 3, 11]. The $p \rightarrow N'$ transition GPDs have been converted to flavor-diagonal GPDs in the proton using relations such as Eq. (4). Vector meson production probes the “unpolarized” GPDs H and E (denoted symbolically by u, d, s, g), pseudoscalar meson production the “polarized” GPDs \tilde{H} and \tilde{E} (denoted by $\Delta u, \Delta d, \Delta s$).

asymmetries, which probe asymptotically subleading amplitudes with transverse (T) virtual photon polarization and offer clues about the reaction mechanism in this sector;

- Ratios of cross sections of similar channels, *e.g.* $K^{*+}/\rho^+, K^0/\pi^0$, etc., which test the flavor structure of the nucleon GPDs.

Specific examples of the use of such observables in strange meson production will be described below.

An important theoretical tool in describing the electroproduction of strange mesons is $SU(3)$ flavor symmetry, which has been extensively tested and used in the analysis of strong reactions and weak decays of strange particles (see Ref. [12] for a recent review). $SU(3)$ symmetry allows one to relate the nucleon to octet hyperon transition matrix element of a quark bilinear operator to a linear combination of diagonal matrix elements in the proton, *e.g.*

$$\langle \Lambda | \bar{s}u | p \rangle = -\frac{1}{\sqrt{6}} [2\langle p | \bar{u}u | p \rangle - \langle p | \bar{d}d | p \rangle - \langle p | \bar{s}s | p \rangle]; \quad (4)$$

in this way one can relate the $N \rightarrow \Lambda$ transition GPDs to the usual flavor–diagonal GPDs in the proton. Table I lists the spin/ﬂavor components of the proton GPD accessible in meson electroproduction with octet baryon final states. Note that $SU(3)$ symmetry breaking effects might be quite different in the valence ($q - \bar{q}$) and sea quark (\bar{q}) distributions (see *e.g.* Ref. [13]); the two are probed in different combinations in the various exclusive channels.

Exclusive meson production can also be studied in processes where the nucleon undergoes a transition to a decuplet baryon, for example the Δ . In such processes the hard scattering process can be thought of as an operator inducing the $N \rightarrow$ resonance transition. When combined with strangeness production, such processes offer interesting possibilities to investigate resonance structure with quantum numbers not accessible in usual photo/electroexcitation. An important theoretical tool in the analysis of such processes is the large- N_c limit of QCD, in which baryons can be described as classical field configurations (solitons), and octet and decuplet baryons appear as different rotational states of the same underlying object [14].

III. TRANSVERSE GLUON IMAGING IN ϕ MESON PRODUCTION

Electroproduction of ϕ mesons is in many ways the simplest hard exclusive process accessible at JLab with 6 and 11 GeV beam energy. Like ρ^0 and ω production, ϕ production proceeds by exchange of vacuum quantum numbers between the target and the projectile, and has a reasonable cross section ($\sim 10^1$ nb for $W = 2 - 3$ GeV and $Q^2 = 1 - 2$ GeV² [15, 16, 17]). However, contrary to the light vector mesons, in ϕ production quark exchange is suppressed, making it a clean probe of the gluon field in the nucleon. Calculations of the ϕ production cross section in the leading–twist approximation, using standard parametrizations of the strange quark and gluon GPDs at a low scale, suggest that ϕ production is dominated by the gluon GPD even at JLab energies (however, the leading–twist approximation cannot reliably predict the absolute cross section) [11]; *cf.* also the analysis of Ref. [18] at smaller values of x_B . Experimentally, the analysis of ϕ meson production is aided by the fact that one can infer the polarization of the produced vector meson from the measurement of its decay angular distribution and use s –channel helicity conservation to extract σ_L , eliminating the need for explicit L/T separation by way of measurements at different beam energies (Rosenbluth separation).

The most interesting ratio observable in ϕ production is the dependence of the differential cross section on the transverse momentum transfer to the target, Δ_\perp ,

$$\frac{d\sigma_L/dt(\Delta_\perp^2)}{d\sigma_L/dt(\Delta_\perp^2=0)} = \text{function}(\Delta_\perp^2, x_B, Q^2), \quad (5)$$

and its change with x_B and Q^2 . Here we have in mind values of the order $|\Delta_\perp| \lesssim 1$ GeV, which carry the information about the transverse structure of the interaction region. The transverse momentum transfer is related to the invariant momentum transfer t by

$$t - t_{\min} = \frac{-\Delta_\perp^2}{1 - \xi^2}, \quad (6)$$

where ξ is 1/2 times the relative longitudinal momentum loss of the target, which in the case of $Q^2 \gg (\text{masses})^2$ is given by

$$\xi = \frac{x_B}{2 - x_B}. \quad (7)$$

QCD factorization predicts that the ratio (5) become independent of Q^2 at fixed x_B . In the subasymptotic regime, the change of the Δ_\perp^2 –dependence with Q^2 reveals the decrease of the transverse size of the interaction region with Q^2 , and thus provides information about the effective transverse size of the $s\bar{s}$ pair forming the ϕ meson (see Fig. 2). At $x_B \ll 10^{-1}$ (HERA, EIC) one has $\xi \ll 1$; moreover, one can neglect t_{\min} in Eq. (6), so that $t \approx -\Delta_\perp^2$, and the Δ_\perp^2 dependence can be identified with the t –dependence of the cross section. At $x_B \gtrsim 10^{-1}$ (JLab) one must distinguish between the Δ_\perp^2 and t dependences when studying the decrease of the transverse size of the interaction region with increasing Q^2 . Also, at $Q^2 \sim \text{few GeV}^2$ it might be necessary to use the exact expression for the longitudinal momentum transfer ξ , including power–suppressed terms of the form $(\text{mass})^2/Q^2$. Observing the expected broadening of the Δ_\perp^2 distribution Eq. (5) with increasing Q^2 and its eventual stabilization (corresponding to shrinkage of the transverse size of the interaction region, *cf.* Fig. 2) affords a simple quantitative test of the approach to the pointlike regime, independent of specific GPD models. We emphasize again that it is the Δ_\perp^2 –dependence at small values, corresponding to $|t - t_{\min}| \lesssim 1$ GeV², which is of interest here, not at values of the order of $|t - t_{\min}| \sim Q^2$.

For sufficiently large Q^2 , when the ratio Eq. (5) has become approximately Q^2 –independent, it can be compared with the ratio of cross sections calculated in terms of GPDs. In the leading–twist approximation,

$$\frac{d\sigma_L/dt(\Delta_\perp^2)}{d\sigma_L/dt(\Delta_\perp^2=0)} = \frac{|\mathcal{F}_g|^2(\xi, t)}{|\mathcal{F}_g|^2(\xi, t_{\min})}, \quad (8)$$

where Δ_\perp^2 and t are related by Eq. (6), and [3]

$$\begin{aligned} |\mathcal{F}_g|^2(\xi, t) &\equiv (1 - \xi^2)|\mathcal{H}_g|^2 \\ &\quad - (\xi^2 + t/4M^2)|\mathcal{E}_g|^2 \\ &\quad - 2\xi^2 \text{Re}(\mathcal{E}_g^* \mathcal{H}_g). \end{aligned} \quad (9)$$

Here \mathcal{H}_g and \mathcal{E}_g are the (complex) leading–twist amplitudes associated with the gluon GPDs,

$$\begin{aligned} \mathcal{H}_g &= e_s^2 \int_{-1}^1 dx H_g(x, \xi, t) \\ &\quad \times \left(\frac{1}{\xi - x + i0} - \frac{1}{\xi + x + i0} \right) \text{ etc.} \end{aligned} \quad (10)$$

Note that the theoretical prediction for the ratio Eq. (8) is independent of the form of the DA of the produced ϕ meson and the details of the treatment of the hard scattering process. The GPDs here are taken at an effective scale $Q_{\text{eff}}^2 < Q^2$, determined by the effective transverse size of the $s\bar{s}$ pair in the production process. The ratio Eq. (8) can be used to constrain the t -dependence of the gluon GPDs, and thus the transverse spatial distribution of gluons in the nucleon, in a largely model-independent manner, free of the uncertainties of present absolute cross section calculations in the GPD approach.

At $x_B \ll 0.1$ the ϕ production cross section is mostly due to the proton helicity-conserving amplitude \mathcal{H}_g [the contribution of the proton helicity-flip amplitude \mathcal{E}_g in Eq. (9) is suppressed], and the amplitude \mathcal{H}_g is dominated by its imaginary part, in which the gluon GPD is sampled at $x = \xi \approx x_B/2$. In this kinematic region Eq. (8) takes the simple form

$$\frac{d\sigma_L/dt(t)}{d\sigma_L/dt(t=0)} = \frac{H_g^2(x = \xi, \xi, t)}{H_g^2(x = \xi, \xi, t=0)}, \quad (11)$$

and the t -dependence of the cross section can directly be interpreted in terms of the t -dependence of the gluon GPD. In this approximation the data for J/ψ , ϕ and ρ^0 production were analyzed in Refs. [5, 21]. The phenomenological interpretation of the data in this region and our theoretical understanding of the t -dependence of the gluon GPD and its change with x are summarized in Ref. [5].

At $x_B \gtrsim 10^{-1}$, the analysis of the ratio Eq. (8) should include the helicity-flip gluon GPD E_g and the presence of a possibly sizable real part of the leading-twist amplitudes. In particular, a real part of the amplitude can arise from the D-term in the gluon GPDs, which is not constrained by the forward limit, and whose magnitude is largely unknown [19]. We note that a sizable gluonic D-term would influence also the leading-twist predictions for ρ^0 production (see Ref. [20] for a discussion of the preliminary CLAS data).

Figure 3 shows the t -dependence of the ϕ production cross section measured in the JLab CLAS experiment [16] (new data were presented recently in Ref. [17]). The curve shows a fit by a t -dependence of the form $d\sigma/dt \propto (1 - t/1.0 \text{ GeV}^2)^{-4}$, corresponding to a dipole form of the t -dependence of H_g in the simplified expression Eq. (11). This form is theoretically motivated by the analogy of the large- x two-gluon form factor with the nucleon axial form factor [21] and describes well the J/ψ photoproduction data from the FNAL E401 / E458 experiments at higher energies and a larger scale Q_{eff}^2 [22]. One sees that it fits well the t -dependence of the CLAS data for $|t| \lesssim 1 \text{ GeV}^2$. This is very encouraging, and supports the universal Δ_{\perp}^2 dependence of these processes implied by the approach to the pointlike regime (assuming the two probe comparable x -values in the gluon GPD).

In the leading-twist approximation, the Fourier transform of the Δ_{\perp} -dependence of the cross section ratio Eq. (5) is related to the impact parameter dependence of

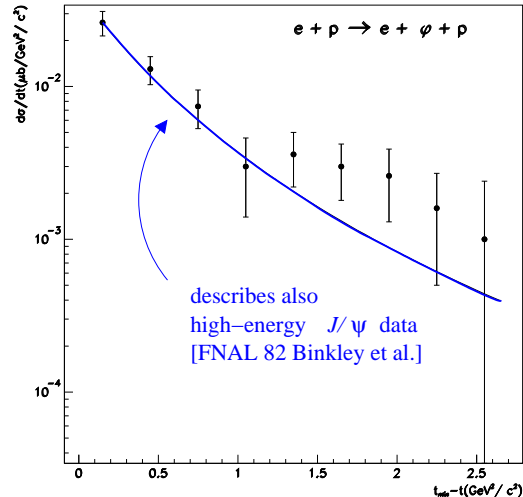


FIG. 3: The differential cross section of exclusive ϕ meson production, $\gamma^*p \rightarrow \phi p$, as a function of t , as measured by JLab CLAS [16]. The curve shows a fit by a t -dependence of the form $d\sigma/dt \propto (1 - t/1.0 \text{ GeV}^2)^{-4}$, corresponding to a dipole form of the t -dependence of the gluon GPD, which describes well the J/ψ photoproduction data from the FNAL E401 / E458 experiments [22].

the GPDs [23, 24]. Provided that Q^2 is sufficiently large to ensure dominance of point-like meson configurations, this can be used to take transverse images of the relevant partonic configurations in the target in these processes. The interpretation of these images is particularly simple at $x_B \ll 0.1$, where one can approximate the gluon GPDs by the “diagonal” one ($\xi = 0$), and the coordinate variable \mathbf{b} measures the distance of the active quark from a fixed (x -independent) transverse center of the nucleon. A more general interpretation, valid in the case $\xi \neq 0$ relevant to JLab experiments, has been described in Ref. [24]. Generally, one expects the transverse size of the relevant partonic configurations in meson production to decrease with increasing x_B (see also the discussion in Refs. [5, 21]). Preliminary results on the x_B -dependence of the t -slope in ρ^0 production have recently been reported by the CLAS Collaboration at JLab [20].

Another interesting observable is the ratio of the ϕ to the ρ^0 and ω production cross sections. If all vector meson production amplitudes were dominated by gluon exchange, the cross section ratio would be independent of x_B ,

$$\frac{\sigma_L(\gamma^*p \rightarrow \phi p)}{\sigma_L(\gamma^*p \rightarrow \rho^0 p)} = \text{const.} \quad (\text{gluon exch.}) \quad (12)$$

Any x_B dependence of the ratio therefore indicates the presence of quark exchange. This test would be particularly instructive at moderately small x_B ($10^{-2} \lesssim x_B \lesssim 10^{-1}$), where the amplitudes are expected to be largely

gluon-dominated but singlet quark exchange still makes a noticeable contribution [18]. In the valence quark region ($x_B \sim 0.2 - 0.5$), where quark exchange is expected to be large, the interpretation of a nontrivial x_B dependence of the ratio is more model-dependent, as the different quark distributions could in principle “conspire” to produce a similar x_B -dependence as gluon exchange over a limited range. Still, the ratio is a good observable for testing the relative importance of singlet quark and gluon exchange at JLab energies. An interesting cross-check would be to analyze also the ratio of ρ^+n to ρ^0p production cross sections; the former is due to nonsinglet quark exchange only, the latter involves both quark and gluon exchange.

Electroproduction of ϕ mesons could also be used to probe the light-quark component ($\bar{u}u, \bar{d}d$) of the ϕ meson, which arises due to $\omega\phi$ and $\rho\phi$ mixing. Specifically, ϕ meson production with $p \rightarrow \Delta^0$ transition,

$$\gamma^*p \rightarrow \phi\Delta^0, \quad (13)$$

requires $I = 1$ and thus light-quark exchange in the t -channel, and couples primarily to the light-quark component of the ϕ . In this example the Δ^0 acts as a “filter” for the quantum numbers transferred to the produced meson. The analysis of this process could also incorporate information on isospin violation in the ϕ meson from the $\phi \rightarrow \omega\pi^0$ decay measured recently in e^+e^- annihilation [25, 26].

IV. HELICITY-FLIP GPD E FROM RECOIL POLARIZATION IN $K^*\Lambda$ PRODUCTION

The “unpolarized” quark GPDs in the nucleon come in the form of two functions, H and E , corresponding to the Dirac and Pauli form factors in the matrix element of the vector current, and related to the possibility of helicity-conserving and helicity-flipping transitions between the nucleon states. The Pauli form factor-type GPD E is of special significance for nucleon structure. Contrary to the Dirac form factor-type GPD H , which at zero momentum transfer coincides with the usual unpolarized quark density, the x -dependence of E is essentially unknown. Only its first moment can be inferred from the nucleon’s anomalous magnetic moment, and it shows that the distribution is sizable and likely to play a significant role in hard exclusive amplitudes. In the impact parameter representation, the function E describes the distortion of the quarks’ longitudinal motion by transverse polarization of the nucleon state [23]. It is also needed as an ingredient to the angular momentum sum rule [27].

Extracting information about the Pauli form-factor type GPD E from experimental data presents a major challenge. In the $N(e, e'\gamma)N$ cross section due to DVCS and Bethe-Heitler interference the contribution of E is suppressed for a proton target, and only experiments with neutron (*i.e.*, nuclear) targets offer reasonable sensitivity. More direct access to E is possible through

leading-twist polarization observables in vector meson production. The transverse target spin dependence of the $\gamma_L^*p \rightarrow \rho_L^0p$ cross section is caused by the interference of nucleon helicity-flip and nonflip amplitudes and given by a term linear in the GPD E [2]. The same term can be accessed by measuring the polarization of the recoiling baryon in scattering from an unpolarized target. Such measurements are possible in $\gamma_L^*p \rightarrow K^{*+}\Lambda$, taking advantage of the “self-analyzing” nature of the Λ — the fact that the orientation of the $\Lambda \rightarrow p\pi^-$ decay plane is almost perfectly correlated with the Λ spin. Such measurements have been widely discussed in connection with semi-inclusive particle production.

More precisely, the differential cross sections for the production of longitudinally polarized vector mesons, $\gamma_L^*(q) + N(p) \rightarrow V_L(q') + N'(p')$, are of the form

$$\sigma_L(\text{target pol.}) = \sigma_0 + (\mathbf{n}\mathbf{S})\sigma_1, \quad (14)$$

$$\sigma_L(\text{recoil pol.}) = \sigma_0 + (\mathbf{n}\mathbf{S}')\sigma'_1, \quad (15)$$

where \mathbf{S} and \mathbf{S}' are the target and recoil spin vectors, and $\mathbf{n} = \mathbf{q}' \times \mathbf{q} / |\mathbf{q}' \times \mathbf{q}|$ is a transverse vector normal to the scattering plane. The general amplitude structure of the process implies that $\sigma'_1 = \sigma_1$ for production of natural parity (1^-) vector mesons (ρ, K^*). In the leading-twist approximation, the relative polarization asymmetries are given by (*cf.* Refs. [2, 3])

$$\begin{aligned} \frac{\sigma_1}{\sigma_0} &= \frac{\sigma'_1}{\sigma_0} \\ &= \frac{|\Delta_\perp| \text{Im}(\mathcal{E}^*\mathcal{H})}{(1 - \xi^2)|\mathcal{H}|^2 - (\xi^2 + t/4M^2)|\mathcal{E}|^2 - 2\xi^2\text{Re}(\mathcal{E}^*\mathcal{H})}, \end{aligned} \quad (16)$$

where \mathcal{H} and \mathcal{E} are the complex leading-twist amplitudes proportional to the GPDs, as defined in Ref. [3] [see also Eq. (10)]. In order to extract this cross section ratio from recoil polarization data one defines the angle, β , of the recoil spin relative to the scattering plane, $(\mathbf{n}\mathbf{S}') = |\mathbf{S}'|\sin\beta$ (with sign as specified by the above definition of \mathbf{n}), and calculates the angular asymmetry of the cross section

$$\begin{aligned} A(\text{recoil pol.}) &\equiv \frac{\int_0^{\pi/2} d\beta \sigma_L(\beta) - \int_{-\pi/2}^0 d\beta \sigma_L(\beta)}{\int_0^{\pi/2} d\beta \sigma_L(\beta) + \int_{-\pi/2}^0 d\beta \sigma_L(\beta)} \\ &= \frac{2|\mathbf{S}'|\sigma_1}{\pi\sigma_0}. \end{aligned} \quad (17)$$

When measuring the asymmetry Eq. (17) in $\gamma_L^*p \rightarrow K^{*+}\Lambda$, the GPDs probed [*cf.* Eq. (16)] are the $p \rightarrow \Lambda$ transition GPDs. They are of interest in themselves, containing useful information about hyperon structure. Alternatively, one can use $SU(3)$ symmetry to relate them to the flavor-diagonal GPDs in the proton, Eq. (4), and in this way extract information about the elusive proton GPD E . Such analysis should eventually include $SU(3)$ breaking both in the meson distribution amplitude

(where it induces an asymmetry of the meson distribution amplitude) as well as in the GPDs. We note that, as in ϕ and ρ^0 production, the cross section for longitudinal photon polarization can be isolated by measuring the $K^* \rightarrow K\pi$ decay and relying on s -channel helicity conservation.

Measurements of recoil polarization in $\gamma_L^* p \rightarrow K^{*+}\Lambda$ could also be done with a polarized target. This combination in principle would allow one to measure the cross sections corresponding to individual helicity amplitudes, making it possible to separate H and E without relying on interference effects.

Another interesting observable is the ratio of ρ^+n and $K^{*+}\Lambda$ production cross sections. The ρ^+n channel involves nonsinglet quark exchange only, and GPD-based calculations of the cross section are free from the uncertainties in the relative strength of gluon and singlet quark exchange affecting the $\rho^0 p$ channel [10, 11]. While not fully model-independent, one can expect the ratio of ρ^+n and $K^{*+}\Lambda$ production cross sections to be more reliably described by GPD-based calculations in the leading-twist approximation than the absolute cross sections.

A rough estimate of the expected $K^{*+}\Lambda/\rho^+n$ cross section ratio can be obtained if we neglect the differences in the final-state masses, use the flavor structure of the production amplitudes as given by $SU(3)$ symmetry (see Table I), assume that $H_u = 2H_d$ and $E_u = 2E_d$, and neglect the contributions from H_s and E_s . With these approximations we obtain

$$\frac{\sigma_L(\gamma^* p \rightarrow K^{*+}\Lambda)}{\sigma_L(\gamma^* p \rightarrow \rho^+n)} \approx \frac{3}{2}, \quad (18)$$

showing that both are of the same order. More detailed calculations have been reported in Ref. [11].

Experiments aiming to study $K^*\Lambda$ production must take into account that the cross section for the $K^*\Sigma^0$ channel is likely to be of comparable magnitude. It will be necessary to separate the two channels, as the Σ^0 decays to Λ via emission of a low-energy photon. This caveat applies also to $K\Lambda$ and $K^*\Sigma^0$ production as discussed in Sec. V.

V. STRANGENESS POLARIZATION IN $K\Lambda$ AND $K\Sigma$ PRODUCTION

Pseudoscalar meson production at high Q^2 probes the “polarized” GPDs \tilde{H} and \tilde{E} , whose first moments are given by the axial and pseudoscalar form factors of the axial vector current operator. At zero momentum transfer the GPD \tilde{H} coincides with the usual polarized quark densities in the nucleon. In this sense, pseudoscalar meson production experiments can probe the spin structure of the nucleon without using target polarization [28, 29].

A special feature of the pseudoscalar GPD \tilde{E} is that it contains a term corresponding to t -channel exchange of pseudoscalar mesons (see Fig. 4), analogous to the “pole

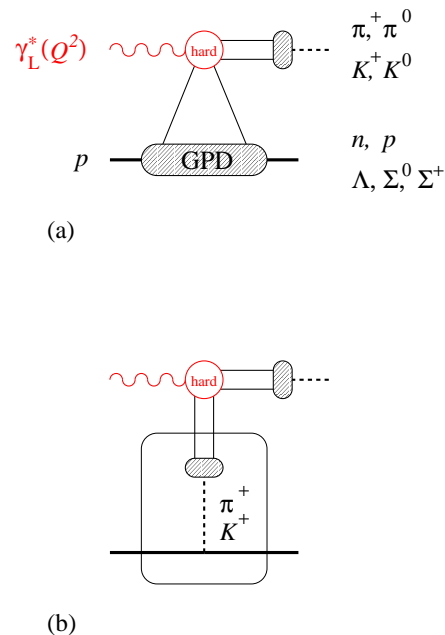


FIG. 4: (a) QCD factorization in pseudoscalar meson production. (b) “Pole” contribution to the GPD \tilde{E} in π^+ and K^+ production. This contribution to the amplitude is equivalent to the virtual photon scattering from a π^+/K^+ emitted by the proton.

term” in the pseudoscalar form factor [28, 29]. In the context of meson production this term corresponds to the process in which a π^+ or K^+ is emitted by the nucleon (with $|t| \sim M_\pi^2, M_K^2$) and interacts with the electromagnetic probe as a whole, via its EM form factor; in fact, this process is the basis of measurements of the π^+ and K^+ form factor in electroproduction from the nucleon. Calculations based on the chiral quark-soliton model of the nucleon [30] show that the π^+ pole term dominates the isovector GPD \tilde{E} at small t and is largely responsible for the π^+ electroproduction cross section at $|t| \sim M_\pi^2$. The K^+ pole term in the $p \rightarrow \Lambda$ GPD is less prominent (because the pole at $t = M_K^2$ is further removed from the physical region $t < t_{\min} < 0$), but it still contributes significantly to the K^+ production cross section [11]. From the point of view of $SU(3)$ symmetry the pole term represents a strong symmetry-breaking effect, as its strength depends on the pole position determined by the π/K mass, and unbroken symmetry would imply $M_\pi = M_K$.

In order to access the spin structure of the nucleon as encoded in the GPD \tilde{H} , and to be able to apply $SU(3)$ symmetry, one needs to separate the “pole” and “non-pole” contributions in pseudoscalar meson production. In the case of pion production this is in principle possible by comparing the π^+n channel with $\pi^0 p$, where the pole contribution is exactly zero because the π^0 is a C -parity eigenstate and does not have a single-photon coupling. However, the two channels involve the isoscalar

($\Delta u + \Delta d$) and isovector ($\Delta u - \Delta d$) GPDs with different coefficients, so that no fully model-independent analysis is possible. In the case of kaon production, the “pole” and “non-pole” contributions could be separated by comparing the $K^+\Sigma^0$ channel, which has a pole contribution, with the $K^0\Sigma^+$ channel, where the pole contribution is not exactly zero but very small, at the level of $SU(3)$ breaking mass effects in the K^0 wave function. An interesting aspect of this comparison is that, when assuming $SU(3)$ symmetry, the $K^+\Sigma^0$ and $K^0\Sigma^+$ GPDs involve the same nonsinglet quark flavor combination ($\Delta d - \Delta s$) of the GPDs, so that the remaining “non-pole” terms in the GPDs can be compared in a relatively model-independent way.

Also of interest would be the comparison of K production with proton and neutron (*i.e.*, nuclear) targets. If the K^+ production amplitude were dominated by the pole term, one would expect that the ratio

$$\frac{\sigma_L(\gamma^*n \rightarrow K^+\Sigma^-)}{\sigma_L(\gamma^*p \rightarrow K^+\Sigma^0)} \quad (19)$$

be independent of x_B . If, however, the amplitude were mainly due to the non-pole term, one would expect significant x_B -dependence, as the x -dependence of the non-pole part of the GPD is governed by the polarized u -quark distribution, which is very different for proton and neutron targets (the u -quark distribution in the neutron is equal to the d -quark distribution in the proton). This study could be complemented by measurement of the corresponding ratio for K^0 production,

$$\frac{\sigma_L(\gamma^*n \rightarrow K^0\Sigma^0)}{\sigma_L(\gamma^*p \rightarrow K^0\Sigma^+)} \quad (20)$$

Because the pole term in K^0 production is suppressed, this ratio is expected to show much stronger x_B dependence than the one for K^+ .

VI. SUMMARY AND OUTLOOK

Ratio observables play a crucial role in the analysis of exclusive meson production experiments at JLab with 6 and 11 GeV beam energy. By studying suitable ratios of cross sections of similar channels, or of cross sections in the same channel at different kinematic points, one can perform numerous model-independent tests of the reaction mechanism, investigate the approach to the point-like regime, and extract limited but specific information about the nucleon GPDs.

The extension to strangeness significantly enhances the reach of the exclusive meson production program at JLab with 11 GeV beam energy. ϕ meson production is an exceptionally clean channel; it probes the gluonic structure of the nucleon already at JLab energies, and the

physical interpretation is closely related that of diffractive vector meson production at higher energies. $K^*\Lambda$ production offers a unique way of studying the helicity structure of the nucleon GPDs through recoil polarization measurements. Experimentally, the requirements of particle identification and energy/momentum resolution in the processes described here vary greatly between the channels and need to be discussed case-by-case.

As already noted, in high- Q^2 meson electroproduction processes of the kind discussed here the cross sections for transition to decuplet baryons are generally of the same order as those for octet baryons. At 11 GeV beam energy, the produced baryon resonance and its decay products will be well-separated from the forward-going meson, so that hadronic final-state interactions are small and both can be studied as independent systems. Many interesting possibilities are connected with the use of hard exclusive processes for the purposes of resonance spectroscopy. Here the meson production process can be thought of as an operator inducing the $N \rightarrow$ resonance transition. An interesting aspect is that these operators can probe flavor/parity quantum numbers not accessible in usual photo/electroexcitation experiments. Also, because the transition operators are nonlocal in the longitudinal direction (they remove a quark at one point and re-insert it at a different longitudinal position), they probe the orbital structure of the resonance wave function in a way different from local currents. The application of high- Q^2 exclusive processes to baryon resonance studies certainly merits further study.

Exclusive meson production could also be studied at higher CM energies ($W \gtrsim 10$ GeV) with a future electron-ion collider (EIC). “Diffractive” channels ($J/\psi, \phi, \rho^0, \text{DVCS}$), which at high Q^2 probe the gluon and singlet quark GPDs, have cross sections which increase with energy and are relatively straightforward to measure. “Nondiffractive” channels ($\pi, K, \rho^+, K^*, \dots$), which probe the spin/flip/charge nonsinglet quark GPDs, have cross sections which decrease with energy and therefore require much higher luminosity. The experimental feasibility of nondiffractive meson production with an EIC is presently being studied; first results have been reported in Ref. [31].

Acknowledgments

Notice: Authored by Jefferson Science Associates, LLC under U.S. DOE Contract No. DE-AC05-06OR23177. The U.S. Government retains a non-exclusive, paid-up, irrevocable, world-wide license to publish or reproduce this manuscript for U.S. Government purposes.

-
- [1] J. C. Collins, L. Frankfurt and M. Strikman, Phys. Rev. D **56**, 2982 (1997) [arXiv:hep-ph/9611433].
- [2] K. Goetze, M. V. Polyakov and M. Vanderhaeghen, Prog. Part. Nucl. Phys. **47**, 401 (2001) [arXiv:hep-ph/0106012].
- [3] M. Diehl, Phys. Rept. **388**, 41 (2003) [hep-ph/0307382].
- [4] A. V. Belitsky and A. V. Radyushkin, Phys. Rept. **418**, 1 (2005) [arXiv:hep-ph/0504030].
- [5] L. Frankfurt, M. Strikman and C. Weiss, Ann. Rev. Nucl. Part. Sci. **55**, 403 (2005) [arXiv:hep-ph/0507286].
- [6] M. Diehl and W. Kugler, Eur. Phys. J. C **52**, 933 (2007) [arXiv:0708.1121 [hep-ph]]; D. Y. Ivanov, L. Szymanowski and G. Krasnikov, JETP Lett. **80**, 226 (2004) [Pisma Zh. Eksp. Teor. Fiz. **80**, 255 (2004)] [arXiv:hep-ph/0407207]; A. V. Belitsky and D. Mueller, Phys. Lett. B **513**, 349 (2001) [arXiv:hep-ph/0105046].
- [7] A. V. Radyushkin, Few Body Syst. Suppl. **11**, 57 (1999) [arXiv:hep-ph/9811225].
- [8] L. Frankfurt, W. Koepf and M. Strikman, Phys. Rev. D **54**, 3194 (1996) [arXiv:hep-ph/9509311].
- [9] S. V. Goloskokov and P. Kroll, Eur. Phys. J. C **42**, 281 (2005) [arXiv:hep-ph/0501242].
- [10] M. Vanderhaeghen, P. A. M. Guichon and M. Guidal, Phys. Rev. D **60**, 094017 (1999) [arXiv:hep-ph/9905372].
- [11] M. Diehl, W. Kugler, A. Schafer and C. Weiss, Phys. Rev. D **72**, 034034 (2005) [Erratum-ibid. D **72**, 059902 (2005)] [arXiv:hep-ph/0506171].
- [12] V. Guzey and M. V. Polyakov, arXiv:hep-ph/0512355.
- [13] J. Lichtenstadt and H. J. Lipkin, Phys. Lett. B **353**, 119 (1995) [arXiv:hep-ph/9504277].
- [14] L. L. Frankfurt, M. V. Polyakov, M. Strikman and M. Vanderhaeghen, Phys. Rev. Lett. **84**, 2589 (2000) [arXiv:hep-ph/9911381].
- [15] D. G. Cassel *et al.*, Phys. Rev. D **24**, 2787 (1981).
- [16] K. Lukashin *et al.* [CLAS Collaboration], Phys. Rev. C **63**, 065205 (2001) [arXiv:hep-ex/0101030].
- [17] J. P. Santoro, E. S. Smith, M. Garcon, M. Guidal, J. M. Laget, C. Weiss and the CLAS Collaboration, arXiv:0803.3537 [nucl-ex].
- [18] S. V. Goloskokov and P. Kroll, Eur. Phys. J. C **53**, 367 (2008) [arXiv:0708.3569 [hep-ph]].
- [19] M. V. Polyakov and C. Weiss, Phys. Rev. D **60**, 114017 (1999) [arXiv:hep-ph/9902451].
- [20] M. Guidal and S. Morrow, arXiv:0711.3743 [hep-ph].
- [21] L. Frankfurt and M. Strikman, Phys. Rev. D **66**, 031502 (2002).
- [22] M. Binkley *et al.*, Phys. Rev. Lett. **48**, 73 (1982).
- [23] M. Burkardt, Int. J. Mod. Phys. A **18**, 173 (2003) [arXiv:hep-ph/0207047].
- [24] M. Diehl, Eur. Phys. J. C **25**, 223 (2002) [Erratum-ibid. C **31**, 277 (2003)] [arXiv:hep-ph/0205208].
- [25] F. Ambrosino *et al.* [KLOE collaboration], arXiv:0707.4130 [hep-ex].
- [26] G. Li, Y. J. Zhang and Q. Zhao, arXiv:0803.3412 [hep-ph].
- [27] X. D. Ji, Phys. Rev. D **55**, 7114 (1997).
- [28] L. Mankiewicz, G. Piller and A. Radyushkin, Eur. Phys. J. C **10**, 307 (1999) [arXiv:hep-ph/9812467].
- [29] L. L. Frankfurt, P. V. Pobylitsa, M. V. Polyakov and M. Strikman, Phys. Rev. D **60**, 014010 (1999) [arXiv:hep-ph/9901429].
- [30] M. Penttinen, M. V. Polyakov and K. Goetze, Phys. Rev. D **62**, 014024 (2000) [arXiv:hep-ph/9909489].
- [31] C. Weiss, Presentation at EIC Collaboration Meeting, Stony Brook University, Stony Brook, NY, 7–8 Dec. 2007, <http://web.mit.edu/eicc/SBU07/>